# Supplementary Information and Figures for "A unified energy optimality criterion predicts human navigation paths and speeds"

Geoffrey L. Brown,[1,2,†] Nidhi Seethapathi,[1,3,†] Manoj Srinivasan[1,4,*]

[1]Mechanical and Aerospace Engineering, the Ohio State University, Columbus, OH 43210
[2]Feinberg School of Medicine, Northwestern University, Chicago, IL 60611
[3]Department of Bioengineering, University of Pennsylvania, Philadelphia, PA 19104
[4]Program in Biophysics, the Ohio State University, Columbus, OH 43210

[*]To whom correspondence should be addressed; E-mail: srinivasan.88@osu.edu.
[†]Equal contribution.

## S1 Optimization methods for behavioral predictions for human path planning

As noted, we use numerical trajectory optimization techniques [1, 2] to determine the energy optimal solutions in Figures 4-6 of the main manuscript, for tasks that require determining the paths as well as speeds during walking. Here, we provide further technical details.

### Optimal path between two points with end-point body orientations

This section corresponds to Figures 4-6 of the main manuscript, in which the goal is go from A to B, with constraints on the initial and final body orientation and, in some cases, velocities. To perform the trajectory optimization, we use the following multiple shooting approach [1]. We consider two kinds of models: non-holonomic and holonomic [3]. In the following, we use the terms 'velocity direction' and 'tangent to the path' interchangeably as they are identical.

#### Non-holonomic: always facing the movement direction

We parameterize the trajectory of the body continuously with $N_{\text{path}}$ grid points, equally spaced in time. Each grid point has the following unknowns representing body state: $(x_b, y_b, \theta_b, v_b, \omega_b)$.

Here, $x_b$ and $y_b$ describe the body trajectory's top view (projection onto the horizontal plane), $v_b = \sqrt{\dot{x}_b^2 + \dot{y}_b^2}$ is the linear speed tangential to the trajectory, $\theta_b$ is both the body orientation and the velocity's angle with the $x$ axis (so that $\dot{x}_b = v_b \cos\theta_b$ and $\dot{y}_b = v_b \sin\theta_b$ due to the non-holonomic constraint), and $\omega_b = \dot{\theta}_b$. The total time $T_{\text{path}}$ is also an unknown.

**Holonomic: not always facing the movement direction**

We parameterize the trajectory of the body continuously with $N_{\text{path}}$ grid points, equally spaced in time. Each grid point has the following unknowns representing body state:
$(x_b, y_b, \theta_b, v_{xb}, v_{yb}, \omega_b)$. Here, $x_b$ and $y_b$ describe the body trajectory's top view (projection onto the horizontal plane), $v_{xb} = \dot{x}_b$ and $v_{yb} = \dot{y}_b$ are the horizontal velocity components, $\theta_b$ is the body angular orientation but need not be aligned with the velocity direction (path tangent). The body angular velocity is $\omega_b = \dot{\theta}_b$. The total time $T_{\text{path}}$ is also an unknown.

**Multiple shooting and constraints**

The following applies to both holonomic and non-holonomic settings, except that for the non-holonomic setting, we have $v_{xb} = v_b \cos\theta_b$ and $v_{yb} = v_b \sin\theta_b$ and for the holonomic setting, $v_{xb}$ and $v_{yb}$ are optimization unknowns. Starting from the $i^{\text{th}}$ grid point $(x_i, y_i, \theta_i)$ with $i < N_{\text{path}}$, we integrate the following equations $\dot{x} = v_{xb}$, $\dot{y} = v_{yb}$, and $\dot{\theta} = \omega$, with $v$ and $\omega$ considered (piecewise) linear, for each time duration $T_{\text{path}}/(N_{\text{path}} - 1)$. Then, we enforce the continuity constraints at the grid points by equating the end state of the integration to the state at the next grid point. We have constraints on the initial values of the body position and body orientation for all comparisons in Figures 4-6. In addition, for predicting the task in Mombaur et al, we constrain the initial body velocity to zero. For predicting Dias et al, we constrain the initial velocity while entering the corridor to energy-optimal straight line walking speed $v_{\text{opt}} = \sqrt{\alpha_0/\alpha_1}$, but leaving this initial velocity as an unknown to be determined by the optimization does not change the results. For predicting Arachavaleta et al, we leave the initial velocity as an unknown to be determined by the optimization, but constraining it to straight line optimal speed as above does not change the results. Body accelerations are limited to maximum values observed during walking [4]. For predicting Dias et al and Arachavaleta et al, we constrain the body trajectory (which corresponds to body center) to be at least a certain distance from the corridor corner or doors, respectively. This clearance value was chosen to be 0.35 based on typical human body dimensions [5]. We minimize the cost function subject to these constraints using nonlinear programming (`fmincon` in `MATLAB`).

**Metabolic cost function**

To compute the energy cost of the walk, we first compute the integral of the steady state metabolic rate over the path, using the appropriate metabolic rate expression for non-holonomic ($\dot{E} = \alpha_0' + \alpha_1' v_b^2 + \alpha_2' \omega^2$) and holonomic ($\dot{E} = \alpha_0' + \alpha_1' v_f^2 + \alpha_2' \omega^2 + \alpha_s v_s^2$). Here, $v_f$ and $v_s$ are components of the velocity along and perpendicular to the direction that the body faces. For

the Arachavaleta et al predictions, we add the cost of an additional 2 meters beyond point B to compute the total energy cost. To add an additional cost for changing speeds, we first compute the kinetic energy in the horizontal plane. Then, we evaluate the cost of the kinetic energy fluctuations as $b_1$ times total positive work (kinetic energy increases) and $b_2$ times total negative work (kinetic energy decreases), where $b_1 = 4$ and $b_2 = 0.85$, corresponding to reciprocals of typical muscle efficiencies, with a multiplicative factor $\lambda = 0.67$ as determined by Seethapathi and Srinivasan [6].

### Turning in an angled corridor

This section provides some additional information on the angled-corridors task from Dias et al. We consider angled corridors with turn angle $\beta$. The length of the corridors on either side of the intersection point is 5 m. The width of the corridors are 1.5 m. The person starts from one end of one corridor and needs to get to the end of the other corridor, having made the turn. The person starts and ends at the middle of the corridor, 0.75 m from the wall. All these constraints are based on the experiments from Dias et al [7], with which we compare our results. As noted earlier, we add wall clearance as an inequality constraint ensuring that the subject does not contact the wall or go too close to the wall.

### Sensitivity bands: Computing walking velocities or trajectories within 1%, 2% or 5% of the energy optimal strategy

In this article, for every calculation of optimal walking, we also compute and plot walking trajectories or velocities that are within 1%, 2%, and/or 5% of the optimum. Here, we briefly describe how these bands are computed using 2% as a placeholder percentage. These computations usually involve solving additional optimization or search problems.

For walking in circles or turning in place (Figures 2 and 3 of the main manuscript), it is a univariate problem of just finding the optimal linear or angular velocity and then finding the appropriate 2% band around it. To compute the 2% band, we first compute the optimal linear or angular velocity and then perform two one-dimensional searches — one above and one below the optimal velocity — to determine the two velocities that have 1.02 times the optimal energy cost. These two velocities determine the 2% band. We found the bands for other percentages analogously.

For the 2% bands for the Arachavaleta et al trajectories (Supplementary Figure S4), for each optimization calculation, we performed at least two additional optimization calculations. These were trajectory optimization problems with all the constraints of the original trajectory optimization problems. In addition, we add a constraint that the energy cost should be 1.02 times the optimal value. Finally, instead of minimizing the energy cost function (as the energy cost value is already constrained), we determine trajectories that have the "least $x$ values", "greatest $x$ values", etc. – that is, minimize $\sum_{i=1}^{N_{\text{path}}} x_i^2$, maximize $\sum_{i=1}^{N_{\text{path}}} x_i^2$, maximize $\sum_{i=1}^{N_{\text{path}}} y_i^2$, etc. These produce trajectories that have the lowest $x$ values (most leftward path on average), largest

$x$ values (most rightward path on average), etc., subject to being 1.02 times the cost. To avoid local minima, when we minimize $\sum_{i=1}^{N_{\text{path}}} x_i^2$, we also constrain the $x_i$ to be entirely to the left of the optimal path (lower in values than that of the optimal path). It is important to note that the trajectories thus obtained need not contain all trajectories within 2% of the cost – nor is it true that every trajectory within this band has a cost within 2% of the optimum. Nevertheless, the bands formed by these computed paths will contain most well-behaved paths within 2% of the optimum; the bands also give us a lower bound on how far paths the paths can be while being within 2% of the optimum energy cost. Thus, the bands give a sense of how flat the energy landscape is near the optimum. Such substantial flatness of the energy landscape – resulting in substantially different trajectories being close in energy costs – may also accommodate time-reversal asymmetry to and from goals [8].

For Mombar et al and Dias et al comparisons, again we generate bands by solving new trajectory optimization problems as above. While we could have solved the problem described in the previous paragraph, we solved different optimization problems based on the comparisons being made. For Dias et al, because the comparisons were for turning velocity, we simply obtained trajectories that minimizes or maximized $\sum v_i^2$ over the path, subject to the energy cost being 1.02 times the optimal cost. For Mombaur et al, we computed trajectories that minimized or maximized the time duration of the task for simplicity while being 1.02 times the optimal cost. For Mombaur et al, an alternative would have been to minimize or maximize maximize $\sum x_i^2$ or $\sum y_i^2$ or $\sum \theta_i^2$ to obtain individual bands for the three state variables being plotted.

In all the holonomic walking calculations, we allow the body orientation to be at most 90 degrees relative to the velocity direction, so that walking backward is ruled out. But backward walking can be allowed easily by having a different coefficient $\alpha_1$ when $|\theta - \beta| > \pi/2$ based on backward walking metabolic cost (known to be higher than forward walking costs and would therefore not be selected except in rare cases).

### Walking in circles

In the main manuscript, to make behavioral predictions about walking in circles, we assumed the non-holonomic form of the metabolic cost function: $\dot{E} = \alpha_0' + \alpha_1' v_b^2 + \alpha_2' \omega^2$, with $v_b = R_b\,\omega$. However, allowing holonomic walking, namely using $\dot{E} = \alpha_0' + \alpha_1' v_f^2 + \alpha_2' \omega^2 + \alpha_s v_s^2$, will result in non-holonomy being selected as optimal, that is, with the sideways velocity $v_s = 0$ or $\beta = \theta$. Thus, the assumption of non-holonomy is internally self-consistent in this case of steady walking in circles.

## S2 Centripetal model: feet movement vs body movement

Consider the body center of mass (mass $m$) moving in a horizontal circle with tangential speed $v_b$ and radius $R_b$. Then, the legs need to not only support the body weight $mg$, but also the centripetal force $mv_b^2/R_b$, where $g$ is acceleration due to gravity. Thus, the effective leg force is

oriented at an angle $\gamma = \tan^{-1}(v_b^2/R_b g)$ to the vertical. That is, the leg should be slanted inward. This standard simple model has been described [9]. This means that the foot travels in a slightly bigger circle than the body. The foot travel radius is then given by $R = R_b + \ell \sin\gamma$, where $\ell$ is the leg length. Further, if the average velocity of the effective foot is $v$, we have $v/R = v_b/R_b$ as the body and the feet go around their circles in the same time duration ($\omega = \omega_b$). Thus, we have the following three equations:

$$\frac{v}{R} = \frac{v_b}{R_b}, \quad \gamma = \tan^{-1}\frac{v_b^2}{gR_b}, \text{ and } \quad R_b = R - \ell\sin\gamma. \tag{1}$$

Given $v, R, g, \ell$, we can compute the corresponding $v_b, R_b$ and $\gamma$ from these three equations. This calculation assumes that the two feet may travel along the same and that the (massless) leg always supports the body.

Our walking-in-circles metabolic experiments constrained the paths that the feet travel on rather than the paths that the body travels in. The original metabolic rate model was in terms of the foot travel variables $v$ and $R$. We converted these to the corresponding body travel variables $v_b$ and $R_b$ and determined the best fit coefficients for $\dot{E} = \alpha_0' + \alpha_1' v_b^2 + \alpha_2' \omega_b^2$. We obtain the coefficient values to be $\alpha_0' = 2.32$ W/kg, $\alpha_1' = 1.28$ W/kg/$(\text{ms}^{-1})^2$, and $\alpha_2' = 1.02$ W/kg/$(\text{rad.s}^{-1})^2$. These coefficients were chosen to ensure that the optimal speeds for straight line walking and turning in place are the same as when computed with the foot-based cost landscape ($\alpha_0/\alpha_1 = \alpha_0'/\alpha_1'$ and $\alpha_0/\alpha_2 = \alpha_0'/\alpha_2'$). This best fit model explained approximately the same fraction of the metabolic cost data variance as the original metabolic model (about 87.5%), and so has about the same explanatory power as the foot-variables based metabolic cost model.

# S3 Biomechanical reasons for the cost of turning

Why does walking with turning cost more energy than walking in a straight line? To be clear, none of our behavioral predictions and explanations of diverse behavioral data rely on mechanistically understanding the sources of the turning cost. Nevertheless, in this paragraph, we briefly consider a few mechanisms.

First, we consider the simplified cost due to centripetal forces described above. From elementary mechanics, we know that while walking in a circle, the body not only experiences gravity, but also centripetal acceleration. This centripetal acceleration is given by $a_n = v_b^2/R_\text{b}$, where $v_b$ is the average body speed and $R_b$ is the radius of the circle described by the body [9]. So, the legs need to provide the centripetal forces in addition to supporting body weight. Given that gravity is vertical and the centripetal acceleration is horizontal, as a first approximation, walking in circles might be viewed as walking under a slightly higher gravity equal to the total acceleration magnitude, namely $\sqrt{g^2 + a_n^2}$. However, for a speed of 1.6 m/s, radius $R = 1$ m, and $g = 9.81$ ms$^{-2}$, the acceleration magnitude $\sqrt{g^2 + a_n^2}$ is greater than gravity $g$ only by about 1.3%. This increase in the 'effective gravity' and the corresponding leg force increase is too small to plausible affect the cost by nearly 50%.

Second, from scaling arguments and small angle approximations [1], it can be shown that similarly low incremental cost for turning is obtained if we consider a simplified point-mass model walking like a 3D inverted pendulum and using a metabolic cost proportional to leg mechanical work and/or leg force. This is because both the mechanical work and the leg force scale approximately with this effective gravity for these simple biped models [1].

As a third simple cost mechanism, we consider that the body is not a point-mass but consists of rigid body segments. The body, as a whole, not only moves in a circle, but also rotates by 360 degrees about the vertical axis. The average angular velocity $\omega$ of the body, treated as a single rigid body, is equal to the revolution rate $\omega = v/R$ of going around the circle. However, this body angular velocity fluctuates substantially within a stride between $\omega_{\min}$ and $\omega_{\max}$. We computed these body angular velocity fluctuations by using marker-based motion capture for six subjects as they walked in circles of different radii and lap durations (Figure S8). Assuming that these body angular velocity fluctuations require additional mechanical work, we derive an additional energy cost of about $0.1\,\omega^2$ in W/kg, if $\omega$ is in rad/s. This estimate is obtained by assuming a body moment of inertia $I_z = 2$ kgm$^2$ and mass $m = 70$ kg. When $\omega_{\max} > \omega_{\min} > 0$, both the positive and negative work per cycle equal $I_z(\omega_{\max}^2 - \omega_{\min}^2)/2$; when $\omega_{\max} > 0$ and $\omega_{\min} < 0$, both the positive and negative work per cycle equal $I_z(\omega_{\max}^2 + \omega_{\min}^2)/2$. Then, the metabolic cost per stride is estimated as $b_1 = 4$ times positive work and $b_2 = 0.85$ times negative work, where again, $b_1$ and $b_2$ are reciprocals of muscle efficiencies. Then, the metabolic cost per time is estimated by dividing by the stride period, also estimated from the motion capture data.

Thus, the costs predicted from simple models is still an order of magnitude smaller than the $0.96\,\omega^2$ obtained in experiment (equation 1 of the main manuscript). Thus, we conclude that an explanation of the additional metabolic cost may require a more detailed model of the human body, for instance, one that better models the body kinematics, the musculature and the muscle metabolic rate, which is well beyond the scope of this article. We reiterate that none of this has any effect on our behavioral predictions and their agreement with data.

# S4 Why smoothness-only objectives predict infinitesimal movement speeds and how speeds scale with distance

We noted in the main manuscript that *pure* smoothness-related objectives [10, 11] such as related to acceleration and its first or second derivatives (termed 'jerk' or 'snap') predict infinitesimal velocities in the absence of additional cost terms. Here, we provide mathematical intuition for why such objectives predict infinitesimal speeds, well-known in the reaching literature [12]. For instance, consider the acceleration based cost:

$$J_a = \int_0^T \dot{v}^2 \, dt$$

or a jerk-based cost

$$J_j = \int_0^T \dddot{v}^2 \, dt$$

for a task that requires you to go from A to B in a straight line, separated by distance $D$. Consider an optimal solution for the position $x_1(t)$ for some given fixed time duration $T_1$, so that $x_1(0) = 0$ and $x_1(T) = D$. We now show that the cost can be lower for a longer time duration $T_2$ (that is, $T_2 > T_1$). To show this, consider a new motion $x_2(t) = x_1(tT_2/T_1)$, so that $x_2(0) = 0$ and $x_2(T_2) = D$. This new motion $x_2(t)$ is a slowed down (time-stretched) version of $x_1(t)$. So we can write both motions in terms of a single function $g(p)$ with $0 \leq p \leq 1$, so that:

$$x_1(t) = g(p) \text{ with } p = t/T_1$$

and

$$x_2(t) = g(p) \text{ with } p = t/T_2.$$

Given that $\ddot{x}_1 = (d^2g/dp^2) \cdot (1/T_1)^2$ and $x_2(t)$ is analogous, we can write the respective acceleration costs as:

$$J_{a1} = \int_0^{T_1} \ddot{x}_1(t)^2 dt = \int_0^1 \left(\frac{d^2g}{dp^2}\right)^2 \frac{1}{T_1^4} T_1 dp = \int_0^1 \left(\frac{d^2g}{dp^2}\right)^2 \frac{1}{T_1^3} dp$$

and

$$J_{a2} = \int_0^1 \left(\frac{d^2g}{dp^2}\right)^2 \frac{1}{T_2^3} dp.$$

Thus, $J_{a2} < J_{a1}$ if $T_2 > T_1$, so that driving duration $T$ to zero is optimal, so infinitesimal speeds are best. Similarly, the jerk cost $J_j$ will be given by

$$J_j = \int_0^1 \left(\frac{d^3g}{dp^3}\right)^2 \frac{1}{T^5} dp,$$

make the inverse dependence on duration only starker, so again infinitesimal speeds are optimal. Further, this general result of infinitesimal speeds being optimal does not rely on the exponent being 2 on the cost integrand; it works for any exponent greater than 1 for both jerk and acceleration costs.

Sometimes, this non-ecological speed prediction is avoided by having a cost for time, equivalent to having an additive constant inside the integrand, for instance in [3], as:

$$\int_0^T (c_0 + c_1 \dot{v}^2) dt \text{ or } \int_0^T (c_0 + c_1 \ddot{v}^2) dt.$$

Because of the $c_0$, the integral has an additional term $c_0 T$, because of which, infinitesimal speed and infinite duration becomes non-optimal and finite duration becomes optimal. However, this fix introduces new issues as it makes the optimal speed quite dependent on the distance

traveled (unless the functional form of the cost is carefully contrived), much more than seen in experiment. For simplicity, define $g(p) = D \cdot h(p)$ in the above reasoning, so that the same overall trajectory $h(p)$ is scaled in both space and time to obtain any particular distance and time. Then, the total acceleration cost will be:

$$c_0 T + \frac{D^2}{T^3} c_3$$

where $c_3$ is the integral $\int h''(p)^2 dp$. Minimizing this quantity with respect to $T$ makes the time duration scale with $\sqrt{D}$, so that speed $v = D/T \sim D/\sqrt{D} \sim \sqrt{D}$. Locomotor speeds do not scale like this with distance [6]. As a consequence, we predict that the cost expression obtained in [3] will predict larger and larger walking velocities for larger and larger distances (well beyond human capability). It can be verified that using jerk cost version produces an even worse dependence of speed on distance ($v \sim D^{0.6\bar{6}}$). However, minimizing a velocity dependent cost (as we have used)

$$\int (c_0 + c_1 v^\gamma) dt$$

for walking a given distance $D$ ensures that the optimal duration $T$ is proportional to $D$, so that the optimal velocity $v$ is independent of distance $D$, as expected.

We have made these arguments in the context of straight line motion, but having analogous terms for angular motion, for instance, $\omega$ and its derivatives results analogous qualitative conclusions regarding turning.

Of course, as noted in the main manuscript, the real objective function may contain acceleration or jerk-related cost terms (perhaps as a proxy for force rate costs) in addition to a velocity dependent costs that we have used. Our critique of these smoothness costs is primarily in their use to the exclusion of metabolic-like costs.

| Model | Bayes Information Criterion | R-squared value |
|---|---|---|
| Default: $\alpha_0 + \alpha_1 v^2 + \alpha_2 \omega^2$ | 48.20 | 88.05 |
| $\ldots + \alpha_3 v$ | 52.86 | 88.06 |
| $\ldots + \alpha_4 \lvert\omega\rvert$ | 50.84 | 88.28 |
| $\ldots + \alpha_5 v \lvert\omega\rvert$ | 52.50 | 88.10 |
| $\ldots + \alpha_3 v + \alpha_4 \lvert\omega\rvert$ | 55.33 | 88.30 |
| $\ldots + \alpha_3 v + \alpha_5 v \lvert\omega\rvert$ | 52.09 | 88.64 |
| $\ldots + \alpha_4 \lvert\omega\rvert + \alpha_5 v \lvert\omega\rvert$ | 57.13 | 88.10 |
| $\ldots + \alpha_3 v + \alpha_4 \lvert\omega\rvert + \alpha_5 v \lvert\omega\rvert$ | 55.78 | 88.75 |

**Table S1:** The default model, namely, $\alpha_0 + \alpha_1 v^2 + \alpha_2 \omega^2$, has the lowest Bayesian Information Criterion (BIC). Picking the model with the lowest BIC allows us to pick a model does not overfit the data, while penalizing model complexity (ie., promoting parsimony). BIC is equivalent to cross-validation procedures asymptotically for linear models [13]. Moreover, we see using a general quadratic relation with six coefficients increases the fraction of variance explained (R-squared value) by less than 0.7%. Recall that we use the absolute value $|\omega|$ here because we did not distinguish between left and right turns in our experiments or analyses, and assume the metabolic rate to be an even function in $\omega$.

# References


[1] M. Srinivasan, Fifteen observations on the structure of energy minimizing gaits in many simple biped models. *J. R. Soc. Interface* **8**, 74-98 (2011).

[2] J. T. Betts, *Practical Methods for Optimal Control Using Nonlinear Programming* (SIAM, 2001).

[3] K. Mombaur, A. Truong, J.-P. Laumond, From human to humanoid locomotionan inverse optimal control approach. *Auton. Robots* **28**, 369–383 (2010).

[4] S. C. Miff, D. S. Childress, S. A. Gard, M. R. Meier, A. H. Hansen, Temporal symmetries during gait initiation and termination in nondisabled ambulators and in people with unilateral transtibial limb loss. *Journal of Rehabilitation Research & Development* **42** (2005).

[5] J. Fruin, *Pedestrian Planning and Design, Revised Edition* (Elevator World, Inc., Alabama, 1987).

[6] N. Seethapathi, M. Srinivasan, The metabolic cost of changing walking speeds is significant, implies lower optimal speeds for shorter distances, and increases daily energy estimates. *Biol. Letters* **11**, 20150486 (2015).

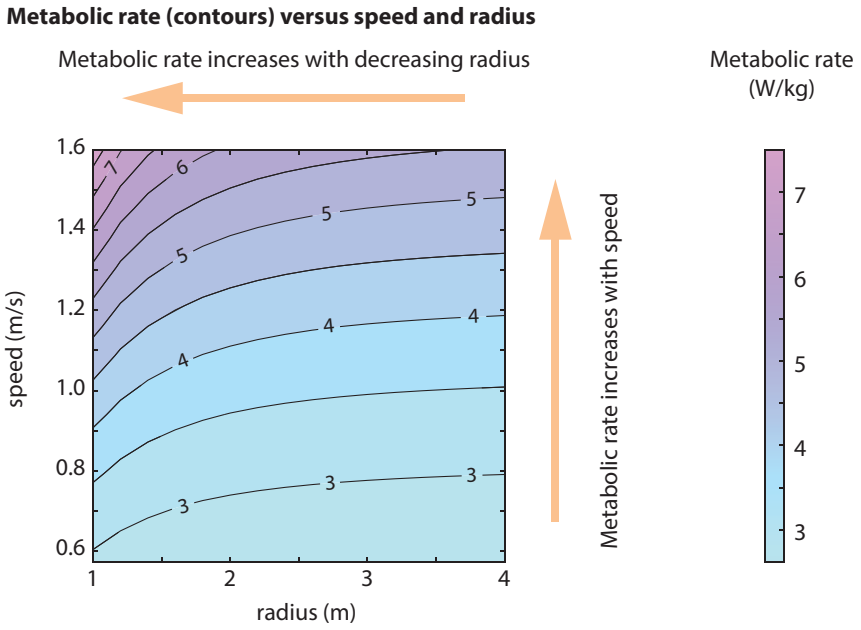


**Figure S1: Metabolic rate contours.** In Figure 1b of the main manuscript, we showed a 3D surface plot of the metabolic rate versus tangential speed and radius. Here, we show a 2D contour plot of the same surface, given by equation 1. The metabolic rate increases with speed for any fixed radius and it increases for decreasing radius for a given speed.

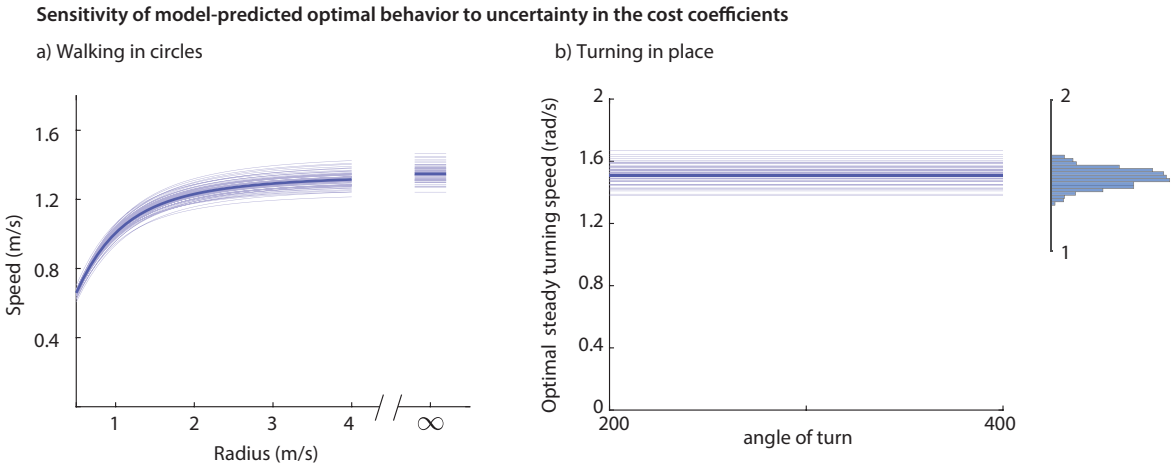


**Figure S2: Optimal walking in circles: Prediction sensitivity to coefficient uncertainty.** Parts a and b of this figure are analogous to Figures 2B and 3C of the main manuscript, respectively. To produce the different curves, we sampled 50 sets of coefficients $\alpha_0$, $\alpha_1$, $\alpha_2$ at random from a normally distributed probability distribution that reflects the uncertainty in these coefficients: this multivariate normal distribution has mean coefficient values used in the main manuscript and covariance equal to the error covariance of the estimated coefficients. The error covariance of the coefficients was obtained using `fitlm` in MATLAB. For each set of coefficients, we computed the preferred walking speeds in circles and preferred steady angular speeds of turning in place, as in the main manuscript, to produce these plots. We note that these optima lie well within the blue bands in the main manuscript, which signify the set of speeds within 1-5% of the optimal speeds.

[7] C. Dias, O. Ejtemai, M. Sarvi, N. Shiwakoti, Pedestrian walking characteristics through angled corridors: An experimental study. *Transportation research record* **2421**, 41–50 (2014).

[8] M. Sreenivasa, K. Mombaur, J.-P. Laumond, Walking paths to and from a goal differ: on the role of bearing angle in the formation of human locomotion paths. *Plos one* **10**, e0121714 (2015).

[9] P. R. Greene, Running on flat turns: experiments, theory, and applications. *J. Biomech. Eng.* **107**, 96 (1985).

[10] Q. Pham, H. Hicheur, G. Arechavaleta, J. Laumond, A. Berthoz, The formation of trajectories during goal-oriented locomotion in humans. ii. a maximum smoothness model. *Eur. J. Neur.* **26**, 2391-2403 (2007).

[11] G. Arechavaleta, J. Laumond, H. Hiceur, A. Berthoz, An optimality principle governing human walking. *IEEE Trans. Robots* **24**, 5-14 (2008).

[12] P. Vivani, T. Flash, Minimum-jerk model, two-thirds power law, and isochrony: converging approaches to movement planning. *Journal of Experimental Psychology: Human Perception and Performance* **21**, 32-53 (1995).

[13] J. Shao, An asymptotic theory for linear model selection. *Statistica sinica* pp. 221–242 (1997).

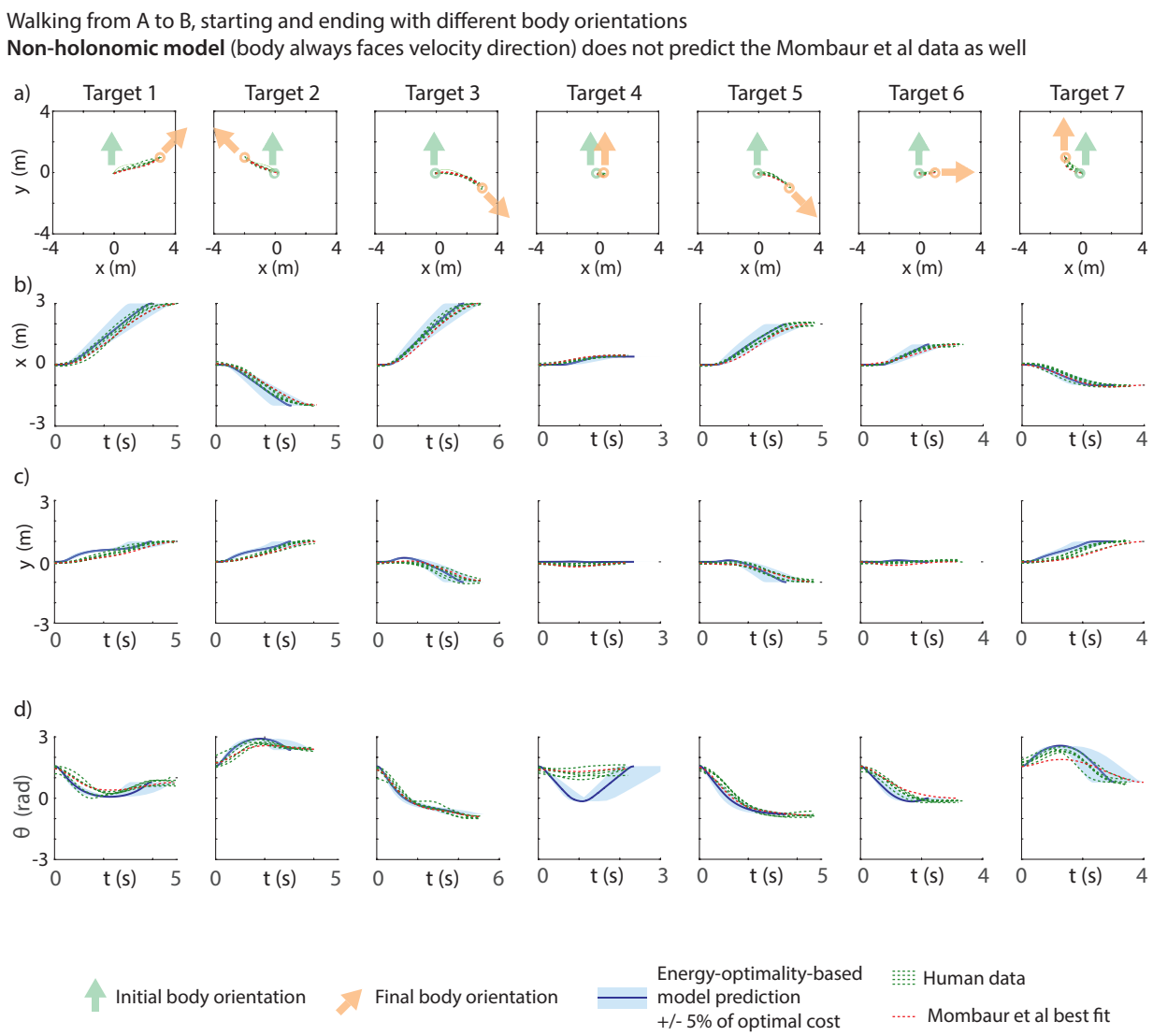


**Figure S3: Prediction vs behavior: Predicting path planning via a non-holonomic model.** a) Mombaur et al [3] asked subjects to walk short distances, starting at rest at point A and ending at rest at point B. The subjects had to start facing one direction (light green arrow) and end facing possibly another direction (orange arrow). b, c, d) The body position $(x, y)$ and body orientation $\theta$ as a function of time. The only difference with the corresponding figure in the main manuscript is that the predictions are based on non-holonomic walking assumptions (facing always in the movement direction). Non-holonomic model predictions are solid dark blue with a light blue band indicating trajectories withing 5% of the optimum cost; experimental data are dashed dark green, and the best-fit model in Mombaur et al [3] is indicated in dashed red line. We see that these non-holonomic model predictions do not agree with data as well as holonomic model predictions in the main manuscript.

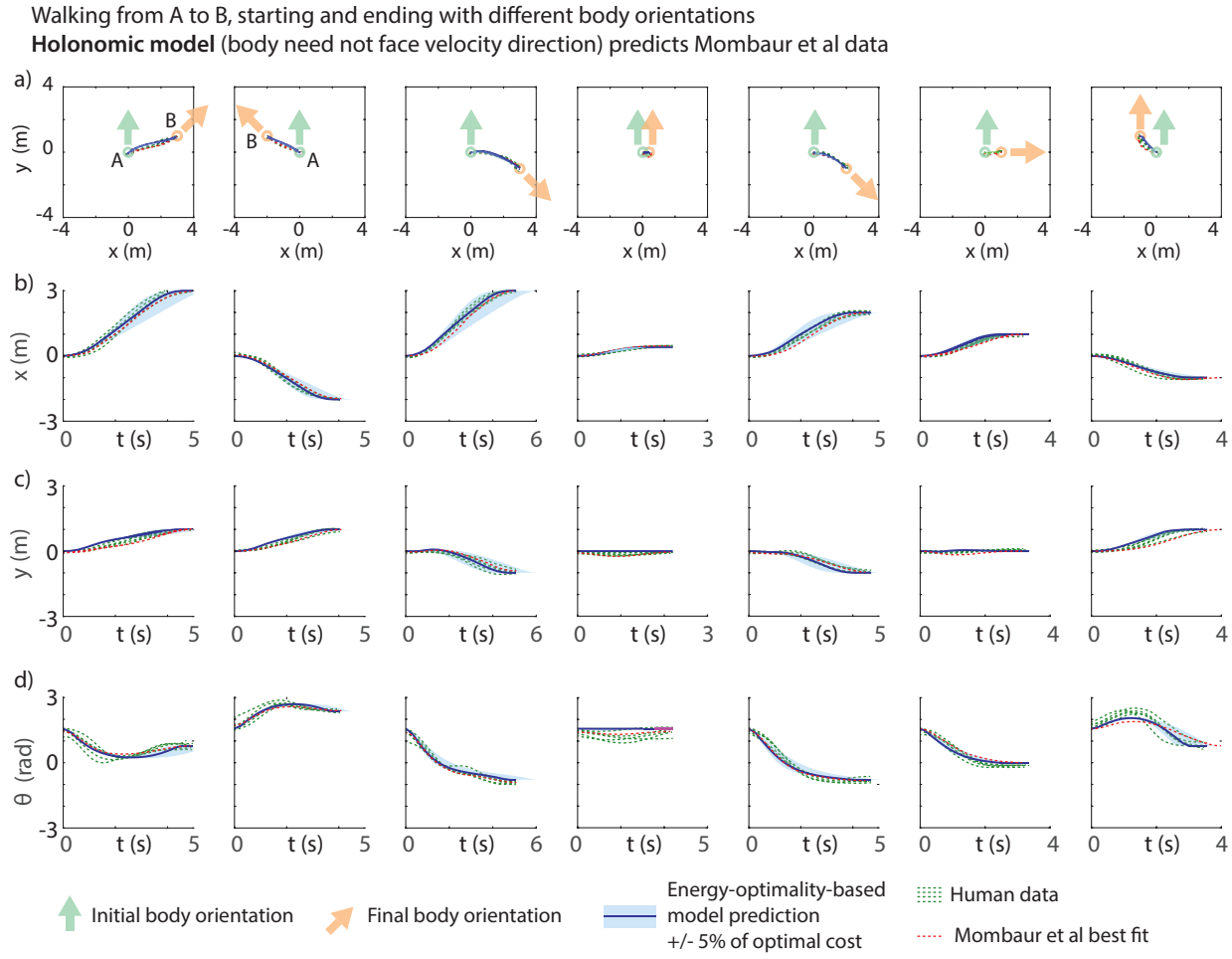


**Figure S4: Prediction vs behavior: Predicting path planning via a holonomic model.** This figure is identical to the corresponding figure in the main manuscript, except for what the initial and final body orientation conditions for the optimization. In the main manuscript, for targets 4 and 7, we used the initial and final body orientation conditions equal to what the subjects started and ended at on average. Here instead, we use the initial and final body orientation conditions equal to that prescribed by the experimenter. Of course, the results of the optimization are very similar to that in the main manuscript except for these small differences – and still predict the observed experimental data well.

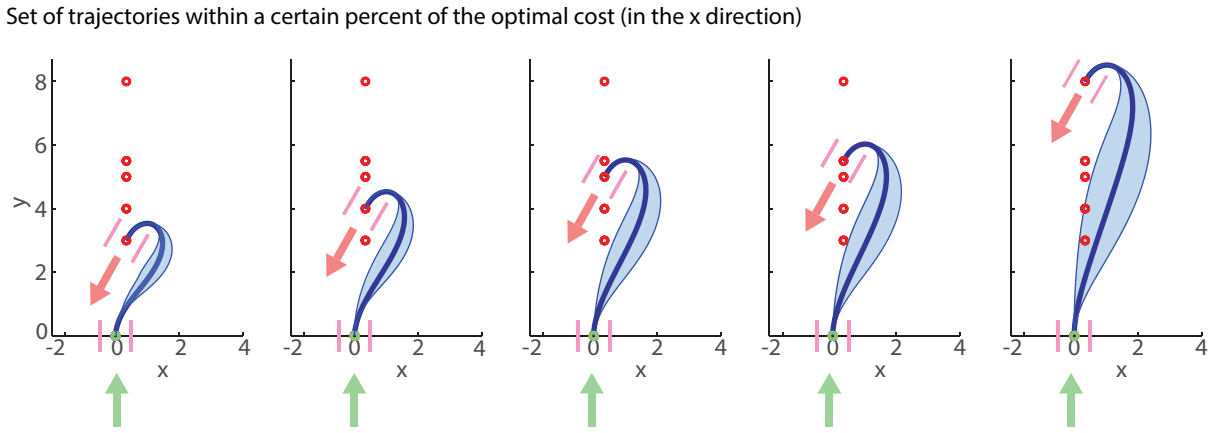


**Figure S5: Path planning via two doorways.** These figures complement the comparison figures for data from Arachavaleta et al in the main manuscript, except now, we show light blue bands around the optimal trajectories. These light blue bands indicate sets of trajectories that are within 2% of the optimal energy costs, in the sense described in the body of this Appendix. We note that the human trajectories are within these bands.

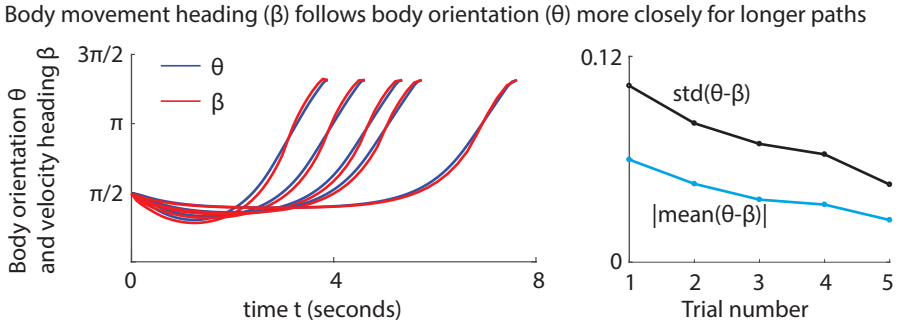


**Figure S6: Body movement heading follows body orientation more closely for longer paths.** a) We show how closely movement direction $\beta$ follows body orientation $\theta$ for the optimal holonomic paths for the five different trials in Figure 6 of the main manuscript (tasks from Arachavaleta et al, as above). b) Mean and standard deviation of the difference between the two orientations decreases with the distance between the initial point and final point. In this plot, the x-axis denotes trial number, with the shortest trial labeled trial 1 and the longest trial labeled trial 5.

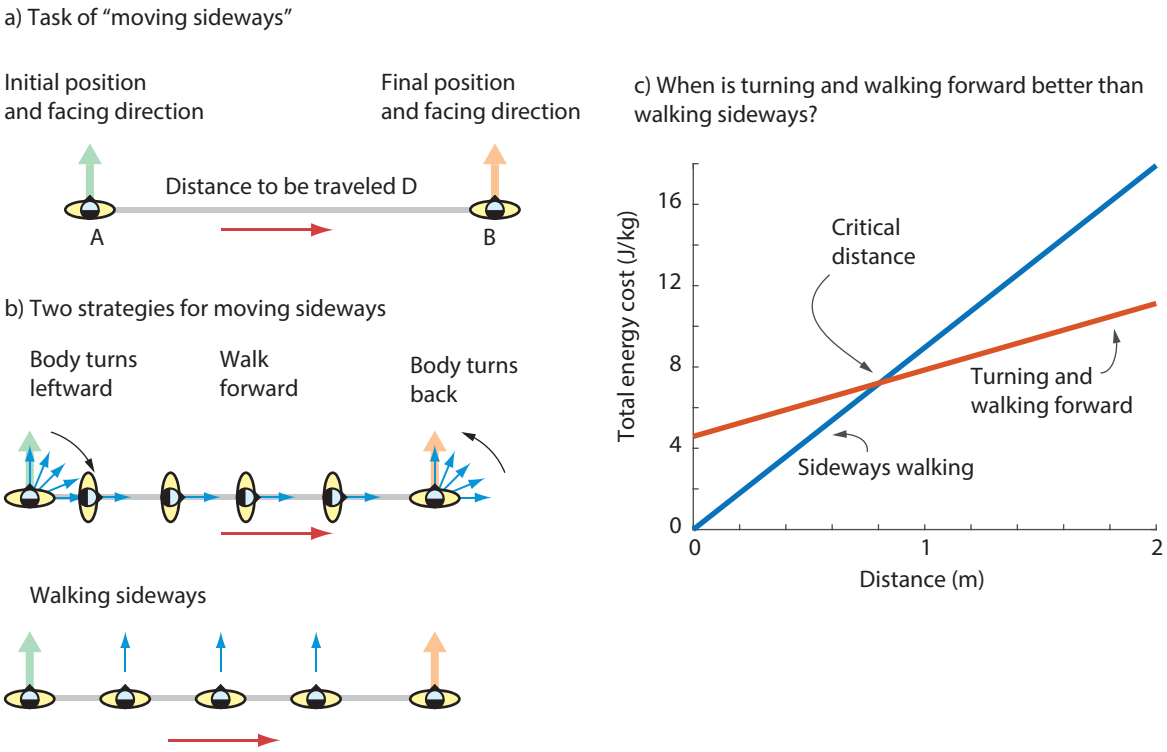


**Figure S7: Stepping sideways vs turning and walking forward.** a) Consider a task in which a human needs to go from A to B, starting and ending facing perpendicular to the line AB. b) Two strategies: sideways walking versus turning and walking forward. c) Metabolic comparison of the two strategies shows a transition in behavior at a critical distance. Indeed, target 4 of the Mombaur et al data is close to this task with $D = 0.4$ and subjects essentially step sideways without much of turning rightward, consistent with the prediction.

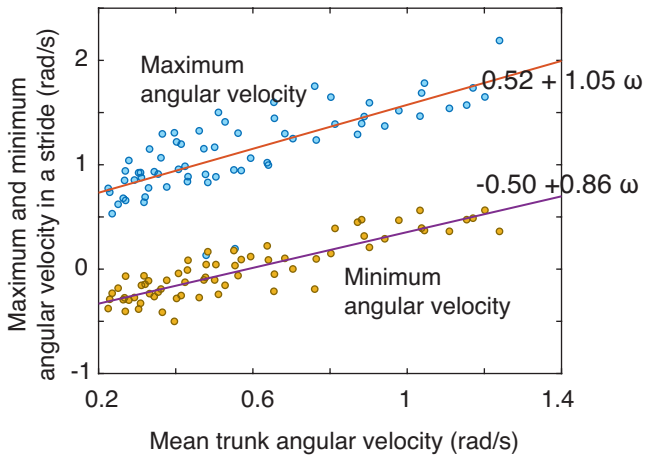


**Figure S8: Trunk angular velocity fluctuations.** While walking in circles, the trunk angular velocity fluctuates about the mean angular velocity $\omega$. Here, the maximum and minimum of such fluctuations are plotted against the mean for 4 radii and at least 4 speeds for all subjects. We see that the fluctuations retain a roughly constant range, slightly increasing with $\omega$.